

# Direct extraction of transversity and its accompanying T-odd distribution from the unpolarized and single-polarized Drell-Yan processes

A.N. Sissakian,<sup>\*</sup> O.Yu. Shevchenko,<sup>†</sup> A.P. Nagaytsev,<sup>‡</sup> and O.N. Ivanov<sup>§</sup>  
*Joint Institute for Nuclear Research, 141980 Dubna, Russia*

The Drell-Yan (DY) processes with unpolarized colliding hadrons and with the single transversely polarized hadron are considered. The possibility of direct (without any model assumptions) extraction of both transversity and its accompanying T-odd parton distribution functions (PDF) is discussed. For DY processes measurements planned at GSI the preliminary estimations demonstrate that it is quite real to extract both transversity and its accompanying T-odd PDF in the PAX conditions.

PACS numbers: 13.65.Ni, 13.60.Hb, 13.88.+e

The advantage of DY process for extraction of PDF, is that there is no need of any fragmentation functions. While the double transversely polarized DY process  $H_1^\uparrow H_2^\uparrow \rightarrow l^+ l^- X$  allows to directly extract the transversity distributions (see ref.[1] for review), in the single polarized DY  $H_1 H_2^\uparrow \rightarrow l^+ l^- X$  the access to transversity is rather difficult since it enters the respective cross-section in the complex convolution with another unknown T-odd PDF (see below). At the same time it is, certainly very desirable to manage to get the transversity PDF from unpolarized and single-polarized DY processes as an alternative possibility. Besides, T-odd PDF are very intriguing and interesting objects in themselves, so that it is very important to extract them too.

The main goal of this paper is to investigate the possibility to completely disentangle PDFs corresponding to the unpolarized and single-polarized DY processes.

Let us first consider the results of ref. [2] for both unpolarized and single-polarized DY processes. In that paper the Collins-Soper frame<sup>1</sup> is used ( see Fig. 3 in ref. [2]), where one deals with three angles  $\theta$ ,  $\phi$  and  $\phi_{S_2}$ . Two angles,  $\theta$  and  $\phi$ , are common for both unpolarized and polarized DY processes. These are the polar and azimuthal angles of lepton pair. Third angle,  $\phi_{S_2}$ , does appear when hadron two is transversely polarized, and this is just the azimuthal angle of  $\mathbf{S}_{2T}$  measured with respect to lepton plane.

We consider here the case of pure transverse polarization of hadron two, so that we put  $\lambda_1 = 0$  and  $|\mathbf{S}_{1T}| = 1$  ( $\lambda_2 = 0$  and  $|\mathbf{S}_{2T}| = 1$  in our notation) in the respective equations of ref. [2] (Eqs. (21) and (22) in ref. [2]) for unpolarized and single polarized cross-sections. Besides, taking into account only the dominating electromagnetic contributions and neglecting (just as in ref. [2]) the ‘‘higher harmonic’’ term containing  $3\phi$  dependence, one gets the following simpli-

fied equations for the QPM unpolarized and single-polarized cross-sections :

$$\begin{aligned} \frac{d\sigma^{(0)}(H_1 H_2 \rightarrow l\bar{l}X)}{d\Omega dx_1 dx_2 d^2\mathbf{q}_T} &= \frac{\alpha^2}{12Q^2} \sum_q e_q^2 \\ &\times \left\{ (1 + \cos^2\theta) \mathcal{F}[\bar{f}_{1q} f_{1q}] + \sin^2\theta \cos(2\phi) \right. \\ &\times \mathcal{F} \left[ (2\hat{\mathbf{h}} \cdot \mathbf{k}_{1T} \hat{\mathbf{h}} \cdot \mathbf{k}_{2T} \right. \\ &\left. \left. - \mathbf{k}_{1T} \cdot \mathbf{k}_{2T}) \frac{\bar{h}_{1q}^\perp h_{1q}^\perp}{M_1 M_2} \right] \right\}, \end{aligned} \quad (1)$$

and

$$\begin{aligned} \frac{d\sigma^{(1)}(H_1 H_2^\uparrow \rightarrow l\bar{l}X)}{d\Omega d\phi_{S_2} dx_1 dx_2 d^2\mathbf{q}_T} &= \frac{\alpha^2}{12Q^2} \sum_q e_q^2 \\ &\times \left\{ (1 + \cos^2\theta) \mathcal{F}[\bar{f}_{1q} f_{1q}] + \sin^2\theta \cos(2\phi) \right. \\ &\times \mathcal{F} \left[ (2\hat{\mathbf{h}} \cdot \mathbf{k}_{1T} \hat{\mathbf{h}} \cdot \mathbf{k}_{2T} - \mathbf{k}_{1T} \cdot \mathbf{k}_{2T}) \frac{\bar{h}_{1q}^\perp h_{1q}^\perp}{M_1 M_2} \right] \\ &+ (1 + \cos^2\theta) \sin(\phi - \phi_{S_2}) \mathcal{F} \left[ \hat{\mathbf{h}} \cdot \mathbf{k}_{2T} \frac{\bar{f}_{1q}^q f_{1q}^{\perp q}}{M_2} \right] \\ &\left. - \sin^2\theta \sin(\phi + \phi_{S_2}) \mathcal{F} \left[ \hat{\mathbf{h}} \cdot \mathbf{k}_{1T} \frac{\bar{h}_{1q}^\perp h_{1q}^\perp}{M_1} \right] \right\}. \end{aligned} \quad (2)$$

Here  $\hat{\mathbf{h}} \equiv \mathbf{q}_T/|\mathbf{q}_T|$ ,  $h_{1q}(x, \mathbf{k}_T^2)$  is the  $k_T$ -dependent transversity distribution, while  $h_{1q}^\perp(x, \mathbf{k}_T^2)$  and  $f_{1T}^{\perp q}(x, \mathbf{k}_T^2)$  are  $k_T$ -dependent T-odd PDFs (see ref. [1] for review). The convolution product is defined [2] as

$$\begin{aligned} \mathcal{F}[\bar{f}_q f_q] &\equiv \int d^2\mathbf{k}_{1T} d^2\mathbf{k}_{2T} \delta^2(\mathbf{k}_{1T} + \mathbf{k}_{2T} - \mathbf{q}_T) \\ &\times [f_q(x_1, \mathbf{k}_{1T}^2) \bar{f}_q(x_2, \mathbf{k}_{2T}^2) + (1 \leftrightarrow 2)]. \end{aligned} \quad (3)$$

Let us first consider the purely unpolarized DY process. Notice that Eq. (1) is very inconvenient in application because of the complicated  $q_T$  and  $k_T$  dependence entering Eq. (1) via the convolution, Eq. (3).

<sup>\*</sup>Electronic address: sissakian@jinr.ru

<sup>†</sup>Electronic address: shev@mail.cern.ch

<sup>‡</sup>Electronic address: nagajcev@mail.desy.de

<sup>§</sup>Electronic address: ivon@jinr.ru

<sup>1</sup> See [1] for detail of the respective kinematics.

To deal with Eq. (1) the model

$$h_{1q}^\perp(x, \mathbf{k}_T^2) = \frac{\alpha_T}{\pi} c_H^q \frac{M_C M_H}{\mathbf{k}_T^2 + M_C^2} e^{-\alpha_T \mathbf{k}_T^2} f_{1q}(x), \quad (4)$$

where  $M_C = 2.3 \text{ GeV}$ ,  $c_H^q = 1$ ,  $\alpha_T = 1 \text{ GeV}^{-2}$  and  $M_H$  is the hadron mass, was proposed in ref. [2]. With a such assumption one then calculates [2, 3] the coefficient  $\kappa \equiv \nu/2$  at  $\cos 2\phi$  dependent part of the ratio

$$R \equiv \frac{d\sigma^{(0)}/d\Omega}{\sigma^{(0)}}, \quad (5)$$

which allows to explain<sup>2</sup> the anomalous  $\cos 2\phi$  dependence [4, 5] of the unpolarized DY cross-section. However, the author of ref. [2] stresses that Eq. (4) is just a ‘‘crude model’’. Besides, Eq. (4) can not help us to extract the quantity  $h_1^\perp$  from the unpolarized DY process.

Thus, to avoid these problems, let us apply the  $\mathbf{q}_T$  weighting approach which was first proposed and applied in refs. [6] and [7] with respect to a particular electron-positron annihilation process and in ref. [8] with respect to semi-inclusive DIS. To use the advantage of  $\mathbf{q}_T$  integration, one should extract from unpolarized DY process the properly integrated over  $\mathbf{q}_T$  ratio (c.f. Eq. (5))

$$\hat{R} = \frac{\int d^2 \mathbf{q}_T [|\mathbf{q}_T|^2 / M_1 M_2] [d\sigma^{(0)}/d\Omega]}{\int d^2 \mathbf{q}_T \sigma^{(0)}}, \quad (6)$$

parametrized as

$$\hat{R} = \frac{3}{16\pi} (\gamma(1 + \cos^2 \theta) + \hat{k} \cos 2\phi \sin^2 \theta), \quad (7)$$

that should be compared<sup>3</sup> with the equation (see refs [2, 4])

$$R = \frac{3}{16\pi} (1 + \lambda \cos^2 \theta + \mu \sin 2\theta \cos \phi + (\nu/2) \cos 2\phi \sin^2 \theta) \quad (\nu \equiv 2\kappa, \lambda \simeq 1, \mu \simeq 0). \quad (8)$$

By virtue of Eq. (1), the coefficient  $\hat{k}$  at  $\cos 2\phi$  dependent part of  $\hat{R}$  reads

$$\begin{aligned} \hat{k} &= \int d^2 \mathbf{q}_T [|\mathbf{q}_T|^2 / M_1 M_2] \\ &\times \sum_q e_q^2 \mathcal{F} [(2\hat{\mathbf{h}} \cdot \mathbf{k}_{1T} \hat{\mathbf{h}} \cdot \mathbf{k}_{2T} - \mathbf{k}_{1T} \cdot \mathbf{k}_{2T}) \frac{\bar{h}_1^\perp h_1^\perp}{M_1 M_2}] \\ &\times \left( \int d^2 \mathbf{q}_T \sum_q e_q^2 \mathcal{F} [\bar{f}_1 f_1] \right)^{-1}, \end{aligned} \quad (9)$$

and, due to the properly chosen weight  $|\mathbf{q}_T|^2$ , the integration over  $\mathbf{q}_T$  leads<sup>4</sup> to the following simple equation for  $\hat{k}$ :

$$\hat{k} = 8 \frac{\sum_q e_q^2 (\bar{h}_{1q}^{\perp(1)}(x_1) h_{1q}^{\perp(1)}(x_2) + (1 \leftrightarrow 2))}{\sum_q e_q^2 (f_{1q}(x_1) f_{1q}(x_2) + (1 \leftrightarrow 2))}, \quad (10)$$

where the standard notation [6, 7, 8]

$$h_{1q}^{\perp(n)}(x) \equiv \int d^2 \mathbf{k}_T \left( \frac{\mathbf{k}_T^2}{2M^2} \right)^n h_{1q}^\perp(x, \mathbf{k}_T^2) \quad (11)$$

for the  $n$ -th moment of  $\mathbf{k}_T$ -dependent PDF is used. Thus, one can see that the numerator of  $\hat{k}$  is factorized out in the simple product of the first moments of  $h_1^\perp$  distributions. This allows to directly extract these quantities from  $\hat{k}$  which should be measured in unpolarized DY. This, in turn (see below), allows to directly extract the transversity distributions  $h_1$  from the single spin polarized DY. Notice that now there is no need in any model assumptions about  $k_T$  dependence of  $h_1^\perp$  distributions.

Let us now consider the single transversely polarized DY process  $H_1 H_2^1 \rightarrow l^+ l^- X$  and define the following single-spin asymmetries (SSA)

$$\begin{aligned} A_{h(f)} &= \\ &\int d\Omega d\phi_{S_2} \sin(\phi \pm \phi_{S_2}) [d\sigma(\mathbf{S}_{2T}) - d\sigma(-\mathbf{S}_{2T})] \\ &\times \left( \int d\Omega d\phi_{S_2} [d\sigma(\mathbf{S}_{2T}) + d\sigma(-\mathbf{S}_{2T})] \right)^{-1}, \end{aligned} \quad (12)$$

where the single-polarized cross-section is given by Eq. (2). It is clear that in the difference  $d\sigma(\mathbf{S}_{2T}) - d\sigma(-\mathbf{S}_{2T})$  only the terms of Eq. (12) containing  $\sin(\phi - \phi_{S_2})$  and  $\sin(\phi + \phi_{S_2})$  survive (and are multiplied by two). Besides, the properly chosen<sup>5</sup> weights:  $\sin(\phi + \phi_{S_2})$  and  $\sin(\phi - \phi_{S_2})$ , allow to separate the contributions containing  $h_1^\perp$  and  $f_{1T}^\perp$  PDF with the result

$$A_h = -\frac{1}{4} \frac{\sum_q e_q^2 \mathcal{F} \left[ \frac{\hat{\mathbf{h}} \cdot \mathbf{k}_{1T} \bar{h}_{1q}^\perp h_{1q}^\perp}{M_1} \right]}{\sum_q e_q^2 \mathcal{F} [\bar{f}_{1q} f_{1q}]}, \quad (13)$$

and

$$A_f = \frac{1}{2} \frac{\sum_q e_q^2 \mathcal{F} \left[ \frac{\hat{\mathbf{h}} \cdot \mathbf{k}_{2T} \bar{f}_{1q}^q f_{1q}^{\perp q}}{M_2} \right]}{\sum_q e_q^2 \mathcal{F} [f_{1q} f_{1q}]}. \quad (14)$$

The asymmetries like  $A_f$  given by Eqs. (12), (14) and their application with respect to Siverson function  $f_{1T}^\perp(x, \mathbf{k}_T^2) \equiv -(M/2|\mathbf{k}_T|) \Delta_{q/H}^N(x, \mathbf{k}_T^2)$  extraction from the data were considered in detail in refs.

<sup>2</sup> Notice that the large values of  $\nu$  cannot be explained by leading and next-to-leading order perturbative QCD corrections as well as by the high twists effects (see [2] and references therein).

<sup>3</sup> Obtaining Eq. (8) one sets [2]  $\lambda = 1$  and  $\mu = 0$  in the most general equation for  $R$  (Eq. (5) in ref. [2]), which is justified [2] by the expectation from next-to-leading order QCD and the data (refs [4, 5]) in the Collins-Soper frame.

<sup>4</sup> The normalization condition  $\int d^2 \mathbf{k}_T f_{1q}(x, \mathbf{k}_T^2) = f_{1q}(x)$  is used (see, for example ref. [1]).

<sup>5</sup> The analogous weighting procedure was applied [9] in the case of transversely polarized SIDIS by the HERMES collaboration.

[10, 11], so that we concentrate here on the asymmetry  $A_h$  given by Eqs. (12) and (13).

Notice that asymmetry  $A_h$  given by Eqs. (12), (13) is inconvenient in application because of the complicated  $q_T$  and  $k_T$  dependence entering the convolution.

So, we again apply the  $q_T$  integration method [6, 7, 8] (see also its application for the SIDIS processes in ref. [9] and for the Siverts PDF extraction from the single polarized DY in ref. [10] ):

$$\hat{A}_h = \frac{\int d\Omega d\phi_{S_2} \int d^2\mathbf{q}_T (|\mathbf{q}_T|/M_1) \sin(\phi + \phi_{S_2}) [d\sigma(\mathbf{S}_{2T}) - d\sigma(-\mathbf{S}_{2T})]}{\int d\Omega d\phi_{S_2} \int d^2\mathbf{q}_T [d\sigma(\mathbf{S}_{2T}) + d\sigma(-\mathbf{S}_{2T})]}, \quad (15)$$

so that one easily gets

$$\hat{A}_h = -\frac{1}{2} \frac{\sum_q e_q^2 [\bar{h}_{1q}^{\perp(1)}(x_1) h_{1q}(x_2) + (1 \leftrightarrow 2)]}{\sum_q e_q^2 [f_{1q}(x_1) f_{1q}(x_2) + (1 \leftrightarrow 2)]}. \quad (16)$$

Thus, one can see that  $\hat{A}_h$  is also factorized in the simple product of  $\bar{h}_1^{\perp(1)}$  and  $h_1$ .

Among variety of DY processes, DY processes with

antiproton ( $\bar{p}p \rightarrow l^+l^-X$ ,  $\bar{p}p^\dagger \rightarrow l^+l^-X$ ,  $\bar{p}^\dagger p^\dagger \rightarrow l^+l^-X$ ) have essential advantage because the charge conjugation symmetry can be applied. Indeed, due to charge conjugation, antiquark PDF from the antiproton are equal to the respective quark PDF from the proton. Thus, Eqs. (10), (16) in the case of  $\bar{p}p$  collisions are rewritten as

$$\hat{k} \Big|_{\bar{p}p^\dagger \rightarrow l^+l^-X} = 8 \frac{\sum_q e_q^2 [h_{1q}^{\perp(1)}(x_1) h_{1q}^{\perp(1)}(x_2) + \bar{h}_{1q}^{\perp(1)}(x_1) \bar{h}_{1q}^{\perp(1)}(x_2)]}{\sum_q e_q^2 [f_{1q}(x_1) f_{1q}(x_2) + \bar{f}_{1q}(x_1) \bar{f}_{1q}(x_2)]}, \quad (17)$$

and

$$\hat{A}_h \Big|_{\bar{p}p^\dagger \rightarrow l^+l^-X} = -\frac{1}{2} \frac{\sum_q e_q^2 [h_{1q}^{\perp(1)}(x_1) h_{1q}(x_2) + \bar{h}_{1q}(x_1) \bar{h}_{1q}^{\perp(1)}(x_2)]}{\sum_q e_q^2 [f_{1q}(x_1) f_{1q}(x_2) + \bar{f}_{1q}(x_1) \bar{f}_{1q}(x_2)]}, \quad (18)$$

where now all PDF *refer to protons*. Neglecting squared antiquark and strange quark PDF contributions to proton and taking into account the quark charges and  $u$  quark dominance at large<sup>6</sup>  $x$ , Eqs. (17) and (18) are essentially given by

$$\hat{k}(x_1, x_2) \Big|_{\bar{p}p^\dagger \rightarrow l^+l^-X} \simeq 8 \frac{h_{1u}^{\perp(1)}(x_1) h_{1u}^{\perp(1)}(x_2)}{f_{1u}(x_1) f_{1u}(x_2)}, \quad (19)$$

and

$$\hat{A}_h(x_1, x_2) \Big|_{\bar{p}p^\dagger \rightarrow l^+l^-X} \simeq -\frac{1}{2} \frac{h_{1u}^{\perp(1)}(x_1) h_{1u}(x_2)}{f_{1u}(x_1) f_{1u}(x_2)}. \quad (20)$$

One can see that the system of Eqs. (19) and (20) has very simple and convenient form in application. Measuring the quantity  $\hat{k}$  in unpolarized DY (Eqs. (6),

(7)) and using Eq. (19) one can obtain the quantity  $h_{1u}^{\perp(1)}$ . Then, measuring SSA, Eq. (15), and using the obtained quantity  $h_{1u}^{\perp(1)}$ , one can eventually extract the transversity distribution  $h_{1u}$  using Eq. (20). Let us stress once again that now there is no need in any model assumptions about  $k_T$  dependence of  $h_1^\perp$  distributions.

In order to obtain squares of  $h_{1u}^{\perp(1)}$  and  $f_{1u}$  in Eqs. (19) and (20), one should consider them at the points<sup>7</sup>  $x_1 = x_2 \equiv x$  (i.e.,  $x_F \equiv x_1 - x_2 = 0$ ), so that

$$h_{1u}^{\perp(1)}(x) = f_{1u}(x) \sqrt{\frac{\hat{k}(x, x)}{8}}, \quad (21)$$

<sup>6</sup> The large  $x$  values is the peculiarity of the  $\bar{p}p$  experiments planned at GSI – see ref. [12]

<sup>7</sup> The different points  $x_F = 0$  can be reached changing  $Q^2$  value at fixed  $s = x_1 x_2 Q^2 \equiv \tau Q^2$ .

and

$$h_{1u}(x) = -4\sqrt{2} \frac{\hat{A}_h(x, x)}{\sqrt{\hat{k}(x, x)}} f_{1u}(x). \quad (22)$$

To estimate the possibility of  $h_{1u}^{\perp(1)}$  and  $h_{1u}$  measurement, the special simulation of DY events with the PAX kinematics [12] are performed. The proton-antiproton collisions are simulated with PYTHIA event generator [13]. Two samples are prepared: for the collider mode (15 GeV antiproton beam colliding on the 3.5 GeV proton beam) and for fixed target mode (22 GeV antiproton beam colliding on an internal hydrogen target). Each sample contains about 100 K pure Drell-Yan events. Notice, that this is just the statistics planned to be achieved by PAX. Indeed (see ref. [12]), the sample for collider mode corresponds to about one year of data-taking with a cross-section of 40 mb and a luminosity of  $2 \times 10^{30} \text{cm}^{-2} \text{s}^{-1}$ . For fixed target mode it can take about three months with a cross-section of 30 mb and a luminosity of about  $10^{31} \text{cm}^{-2} \text{s}^{-1}$ .

Unfortunately, the original PYTHIA generator we deal with does not reproduce the corresponding to DY experiments [4, 5] nontrivial  $q_T$  and  $x$  dependencies of the quantity  $\nu$  entering Eq. (8). So, to estimate the possibility of  $h_{1u}^{\perp(1)}$  and  $h_{1u}$  measurement, one should properly introduce these dependencies in accordance with the existing experimental data. To this end we apply the commonly used Monte-Carlo method based on weighting of the kinematical events. To apply the weighting procedure in our case, we just ascribe to each event the weight  $w = R$  which, in accordance with the data [4, 5], is given by Eq. (8), where  $\lambda \simeq 1$ ,  $\mu \simeq 0$  and  $\nu$  has nontrivial  $q_T$  and  $x$  dependencies. The  $q_T$  dependence of  $\nu$  is taken from refs. [2, 3] – Eq. (49) in ref. [2] and Eq. (21) in ref. [3], and this  $q_T$  dependence properly fits the existing experimental data [4, 5]. However, in refs. [2, 3] (where the simplified Boer's model is applied) there is no (important and corresponding to DY experiments [4, 5])  $x$ -dependence of  $\nu$  at all, so that we take this dependence from ref. [4].

To check the validity of the angular distribution analysis of the weighted events we reconstruct the  $q_T$  and  $x_1$  dependencies of  $\nu$ . The results are shown in Figs. 1, 2. One can see a good agreement<sup>8</sup> between input (solid lines) and reconstructed (points with error bars) values.

Thus, applying the above described weighting procedure, our simulations reproduce the nontrivial angular dependence of  $R$  with  $q_T$ - and  $x$ -dependent  $\nu$ . These dependencies are in accordance with the respective input dependencies obtained in experiments on

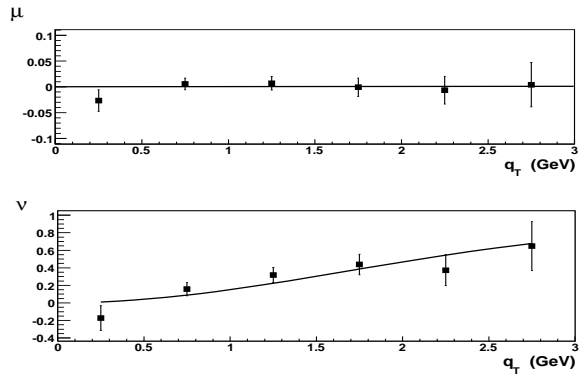


FIG. 1: Reconstructed from simulations (fixed target mode) quantities  $\mu$  and  $\nu$  versus  $q_T$  in comparison with the input (corresponding to experimental data) dependencies (solid lines).

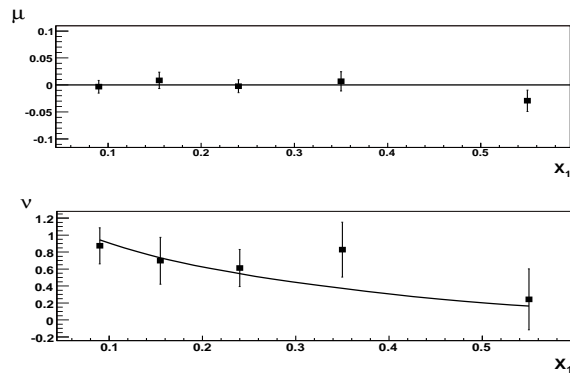


FIG. 2: Reconstructed from simulations (fixed target mode) quantities  $\mu$  and  $\nu$  versus  $x_1$  in comparison with the input (corresponding to experimental data) dependencies (solid lines).

DY [4, 5]. Now it is straightforward to reconstruct the  $q_T$ -weighted quantity  $\hat{R}$  (Eq. 6) and, consequently,  $\hat{k}$  (Eq. 7). The results are shown in Fig. 3. The values of  $\hat{k}$  at averaged  $Q^2$  for both modes are found to be  $1.2 \pm 0.2$  for collider mode and  $1.0 \pm 0.2$  for fixed target mode.

The quantity  $h_{1u}^{\perp(1)}$  is reconstructed from the obtained values of  $\hat{k}$  using Eq. (21) with  $x_F = 0 \pm 0.04$ . The results are shown in Fig. 4. The obtained magnitudes of  $h_{1u}^{\perp(1)}$  are in accordance (in order of value) with the respective magnitudes obtained with the model (4) for  $h_{1u}^{\perp(1)}(x, \mathbf{k}_T)$ . Indeed, for example for the collider mode ( $Q_{average}^2 \simeq 9 \text{ GeV}^2$ , so that  $x_1 \simeq x_2 \simeq 0.2$  at the point  $x_F \simeq 0$ ) the results from the simulations and from the model (4) are  $h_{1u}^{\perp(1)} \simeq 1$  and  $h_{1u}^{\perp(1)} \simeq 0.5$ , respectively.

Using the obtained magnitudes of  $h_{1u}^{\perp(1)}$  we estimate the expected SSA given by Eq. (20). The results are shown in Figs. 5 and 6. For estimation of  $h_{1u}$  entering SSA together with  $h_{1u}^{\perp(1)}$  (see Eq. (20)) we follow the

<sup>8</sup> As an additional check of our analysis validity, we reproduce the input zero value of  $\mu$ .

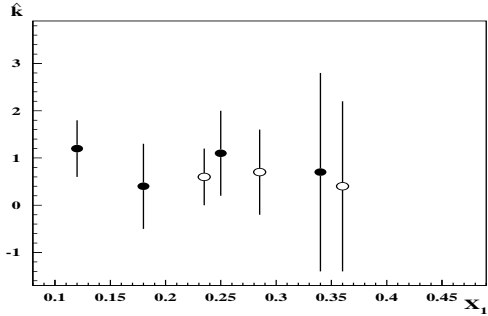


FIG. 3:  $\hat{k}$  versus  $x_1$  at  $x_F \simeq 0$ . Data is obtained with MC simulations for collider (closed circles) and for fixed target mode (open circles). For better visibility (to avoid overlapping) the points for collider (fixed target) mode are shifted 0.01 to the left (right) along the  $x$ -axis.

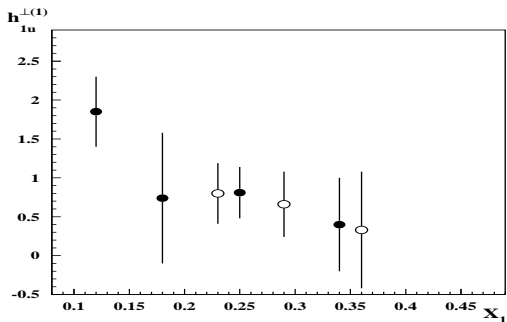


FIG. 4:  $h_{1u}^{\perp(1)}$  versus  $x_1$  at  $x_F \simeq 0$ . Data is obtained with MC simulations for collider (closed circles) and for fixed target mode (open circles). For better visibility (to avoid overlapping) the points for collider (fixed target) mode are shifted 0.01 to the left (right) along the  $x$ -axis.

procedure of ref. [14] and use (rather crude) “evolution model” [2, 14], where there is no any estimations of uncertainties. That is why in (purely qualitative) figures 5 and 6 we present the solid curves instead of points with error bars. To obtain these curves we reproduce  $x$ -dependence of  $h_{1u}^{\perp(1)}$  in the considered region, using the Boer’s model, Eq. (4), properly numerically corrected in accordance with the simulation results.

To estimate the measurability of the quantities we deal with, it is relevant to estimate the upper bounds on  $h_1$ ,  $h_1^{\perp(1)}$  and then on  $\hat{k}$  and  $\hat{A}_h$ . Obtaining  $h_{1u}^{\perp(1)}$  and  $h_{1u}$  one deals with Eqs. (19), (20) applied at the points  $x_1 \simeq x_2 \simeq \sqrt{Q^2/s}$ , so that we perform the estimation of the upper bounds on  $\hat{k}$  and  $\hat{A}_h$  at the points  $x_F \simeq 0$  corresponding to the average  $Q^2$  values for both collider and fixed target

modes. The maximally allowed value of  $h_1^{\perp(1)}$  can be found operating just as it was done with respect to the quantity  $f_{1T}^{\perp(1)q}$  (first moment of the Sivers function) in ref. [10]. To this end we first apply the inequality<sup>9</sup> [15]  $(|\mathbf{k}_T|/M)h_1^{\perp}(x, \mathbf{k}_T^2) \leq f_1(x, \mathbf{k}_T^2)$ . Then, using the estimation (see ref. [10] and references therein)  $\langle k_T \rangle \simeq 0.8 \text{ GeV}$  one easily gets the upper bound on  $h_{1u}^{\perp(1)}$ :  $h_{1u}^{\perp(1)} \lesssim 0.4f_{1u}(x)$ . On the other hand, maximally allowed value of  $h_{1u}$  can be found using the Soffer [16] inequality  $|h_{1u}| \leq (f_{1u} + g_{1u})/2$ . For the PAX kinematics  $s = 43 \text{ GeV}^2$ ,  $Q_{average}^2 \simeq 5 \text{ GeV}^2$  for the fixed target mode and  $s = 215 \text{ GeV}^2$ ,  $Q_{average}^2 \simeq 9 \text{ GeV}^2$  for the collider mode. Thus, at the point  $x_F = 0$  we deal with,  $x_1 \simeq x_2 \simeq 0.3$  and  $x_1 \simeq x_2 \simeq 0.2$  for the fixed target and collider modes, respectively. Then, the inequalities on  $h_{1u}$  and  $h_{1u}^{\perp(1)}$  give<sup>10</sup>  $h_{1u(max)} \simeq 1.5$  ( $f_{1u} = 1.9$ ,  $g_{1u} = 1.0$ ) and  $h_{1u(max)}^{\perp(1)} \simeq 0.8$  for fixed target mode while  $h_{1u(max)} \simeq 2.3$  ( $f_{1u} = 3.1$ ,  $g_{1u} = 1.5$ ) and  $h_{1u(max)}^{\perp(1)} \simeq 1.2$  for collider mode. Using these estimations of  $h_{1u(max)}$  and  $h_{1u(max)}^{\perp(1)}$  in Eqs. (19), (20) it is straightforward to obtain the maximally allowed values of  $\hat{k}$  and  $\hat{A}_h$ :  $\hat{k}_{(max)} \simeq 1.4$  and  $|\hat{A}_{h(max)}| \simeq 0.17$  for fixed target mode while  $\hat{k}_{(max)} \simeq 1.2$  and  $|\hat{A}_{h(max)}| \simeq 0.14$  for collider mode. One can see that obtained estimations of upper bounds on  $h_{1u}^{\perp(1)}$ ,  $\hat{k}$  and  $\hat{A}_h$  are in accordance with the results presented by Figs. 3-6.

Looking at the (preliminary) estimations presented by Figs. 3 and 4, one can conclude that the quantities  $\hat{k}$  and  $h_{1u}^{\perp(1)}$  are presumably measurable in most of the considered  $x$ -region. At the same time, looking at Figs. 5 and 6 one can see that for both modes SSA  $\hat{A}_h$  is estimated to be about 6-8%. On the other hand, as it was argued in Ref. [12] (see section “Single Spin asymmetries and Sivers Function”, p. 25), the studied in ref. [10] SSA  $A_{UT}^{\sin(\phi - \phi_S) \frac{q_T}{M_N}}$  of order 5-10% can be measured by PAX. It is obvious that studied in this paper SSA  $\hat{A}_h$ , weighted with  $\sin(\phi + \phi_S)$  and the same weight  $q_T/M_N$ , is absolutely analogous to SSA  $A_{UT}^{\sin(\phi - \phi_S) \frac{q_T}{M_N}}$ , so that it is clear that if  $A_{UT}^{\sin(\phi - \phi_S) \frac{q_T}{M_N}}$  of 5-10% is measurable, then  $\hat{A}_h$  of 6-8% is measurable too.

Thus, it is shown that it is possible to directly extract the transversity and its accompanying T-odd PDF from the unpolarized and single polarized DY processes with antiproton participation. It is of importance that there is no need in any model assump-

<sup>9</sup> This inequality is directly obtained by relaxing the bound Eq. (16) in ref. [15] (eliminating the unknown distribution in that bound).

<sup>10</sup> Performing these estimations we use GRV2000LO parametrization [17] for  $g_{1u}$  and GRV98LO parametrization [18] for  $f_{1u}$ .

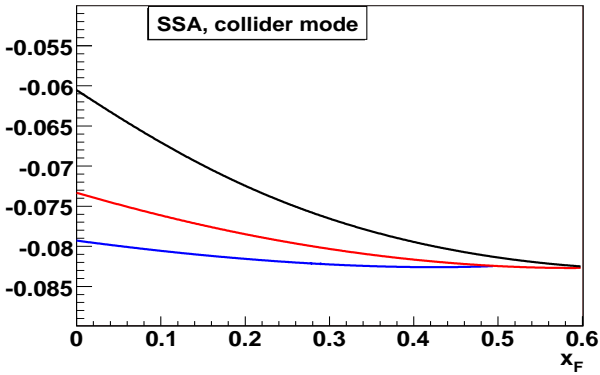


FIG. 5: SSA given by Eq. (20) versus  $x_F$  for collider mode for three values of  $Q^2$ :  $50 \text{ GeV}^2$  (lower curve),  $25 \text{ GeV}^2$  (middle curve) and  $9 \text{ GeV}^2$  (upper curve).

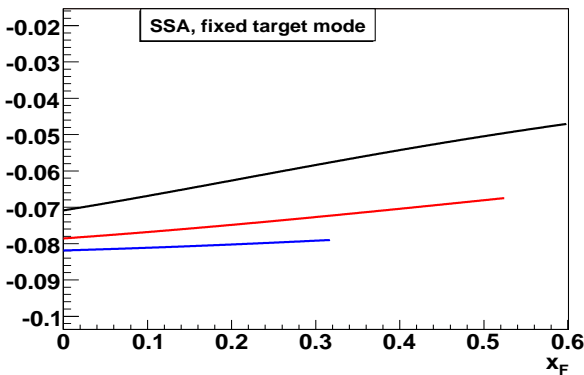


FIG. 6: SSA given by Eq. (20) versus  $x_F$  for fixed target mode for three values of  $Q^2$ :  $16 \text{ GeV}^2$  (lower curve),  $9 \text{ GeV}^2$  (middle curve) and  $4 \text{ GeV}^2$  (upper curve).

tions about  $k_T$  dependence of  $h_1^\perp$ . One can directly extract both  $h_1$  and first moment of  $h_1^\perp$  from the single-polarized and unpolarized DY processes, since these quantities enter the measured  $\hat{k}$  and SSA  $A_h$  in the form of simple product instead of complex convolution. The preliminary estimations for PAX kinematics show the possibility to measure both  $\hat{k}$  and SSA  $\hat{A}_h$  and then to extract the quantities  $h_1^{\perp(1)}$  and  $h_1$ . Certainly, the estimations of  $\hat{k}$  and  $\hat{A}_h$  magnitudes obtained in this paper are very preliminary and show just the order of values of these quantities. For more precise estimations one needs the Monte-Carlo generator more suitable for DY processes studies (see, for example, ref. [3]) than PYTHIA generator which we used (with the proper weighting of events) here.

Notice, that it is straightforward to properly modify the procedure discussed in this paper to DY processes:  $\pi^- p \rightarrow \mu^+ \mu^- X$  and  $\pi^- p^\uparrow \rightarrow \mu^+ \mu^- X$ , which could be studied [19] in the COMPASS experiment at CERN.

The authors are grateful to M. Anselmino, R. Bertini, O. Denisov, A. Efremov, A. Kacharava, V. Krivokhizhin, A. Kulikov, P. Lenisa, A. Maggiora, A. Olshevsky, G. Piragino, G. Pontecorvo, F. Rathmann, I. Savin, M. Tabidze, O. Teryaev and W. Vogelsang for fruitful discussions. The work of O.S. and O.I. was supported by the Russian Foundation for Basic Research (project no. 05-02-17748).

- 
- [1] V. Barone, A. Drago, and P.G. Ratcliffe, Phys. Rep. **359**, 1 (2002), hep-ph/0104283
  - [2] D. Boer, Phys. Rev. D **60**, 014012 (1999).
  - [3] A. Bianconi, M. Radici Phys. Rev. D **71**, 074014 (2005).
  - [4] J.S. Conway et al, Phys. Rev. D **39**, 92 (1989).
  - [5] S. Falciano et al., NA10 Collab., Z. Phys. C **31**, 513 (1986); M. Guanziroli et al., Z. Phys. C **37**, 545 (1988).
  - [6] D. Boer, R. Jakob, P. J. Mulders, Nucl. Phys. B **504**, 345 (1997)
  - [7] D. Boer, R. Jakob, P. J. Mulders, Phys. Lett. B **424**, 143 (1998)
  - [8] D. Boer, P. J. Mulders, Phys. Rev. D **57**, 5780 (1998)
  - [9] HERMES collaboration (A. Airapetian et al), Phys. Rev. Lett. **84**, 4047 (2000); Phys. Rev. D **64**, 097101 (2001); Phys. Lett. B **562**, 182 (2003); Phys. Rev. Lett. **94**, 012002 (2005).
  - [10] A.V. Efremov et al, Phys. Lett. B **612**, 233 (2005).
  - [11] M. Anselmino, U. D'Alesio, F. Murgia, Phys. Rev. D **67**, 074010 (2003).
  - [12] V. Barone et al., PAX Collaboration, "Antiproton-Proton Scattering Experiments with Polarization", Julich, April 2005, accessible electronically via [http://www.fz-juelich.de/ikp/pax/public\\_files/tp\\_PAX.pdf](http://www.fz-juelich.de/ikp/pax/public_files/tp_PAX.pdf)
  - [13] T. Sjostrand et al., hep-ph/0308153.
  - [14] M. Anselmino, V. Barone, A. Drago, N.N. Nikolaev, Phys. Lett. B **594**, 97 (2004).
  - [15] A. Bacchetta, M. Boglione, A. Henneman, P.J. Mulders, Phys. Rev. Lett. **85**, 712 (2000); hep-ph/9912490.
  - [16] J. Soffer, Phys. Rev. Lett. **74**, 1292 (1995)
  - [17] M. Gluck, E. Reya, M. Stratmann, W. Vogelsang, Phys. Rev. D **63**, 094005 (2001).
  - [18] M. Gluck, E. Reya, A. Vogt, Eur. Phys. J. C **5**, 461 (1998).
  - [19] R. Bertini et al., private communication.